Cellular Model of Room Evacuation Based on Occupancy and Movement Prediction

Pavel Hrabák[1,⋆], Marek Bukáček[1], Milan Krbálek[1]

Faculty of Nuclear Sciences and Physical Engineering, Czech Technical University in Prague, Czech Republic
{pavel.hrabak, bukacma2, milan.krbalek}@fjfi.cvut.cz

Abstract. The rule-based CA for simulating the evacuation process of single room with one exit is presented. Analogically to the Floor-Field model, the presented model is based on the movement on rectangular lattice, driven by the potential field generated by the exit. Several ideas of decision-making allowing the agent to choose an occupied cell are implemented, to reflect the observed behaviour in high densities. The velocity of pedestrians is represented by the updating frequency of the individuals. To calibrate model parameters, an experiment "leaving the room" was organized. Based on the observed behaviour, the influence of parameters is discussed and several modifications are suggested.

Keywords: Evacuation model; shape of pedestrian cloud; movement prediction.

1 Introduction

The model presented in this article is primarily designed to support the experimental study of pedestrian cloud formation in front of the exit during non-panic evacuation of single room without obstacles. Such a model should reflect important features observed in the real system ([6]). Several ways of describing pedestrian interaction by the so called "social force" appeared in [3], being suitable not only for evacuation purposes ([2]), but for other crowd features as well ([13]). Such approach is very attractive but mostly not applicable for fast, ideally real-time simulations. In this case, the computational power of Cellular Automata should be used. For elaborate summary of CA phenomena in pedestrian dynamics we refer the reader to [10] or [12].

The inspiration for the model presented in this article is the Floor-Field model ([5], [11]) and its implementation in F.A.S.T ([9], [10], [13]). Similarly to this model, the potential field is considered, but unlike these models the desired line formation is reached using "bounds" rather then the dynamical field. This is closely related to the possibility of choosing an occupied cell ([4]). To handle the problem of the diagonal movement symmetrization (discussed e.g. in [7], [9], [14], or [18]) the time penalization of diagonal movement is implemented.

⋆ Corresponding author

Inspired by [8], [16], and [17], simple movement prediction is taken into account. Furthermore, essential change in the potential iso-curves solves elegantly the problem of wall repulsion mentioned in [1].

2 Description of the Model

The presented model is designed to describe and simulate the following situation: Consider a rectangle room with one exit (see Figure 1), containing given number of persons. People inside the room are motivated to exit the room as fast as possible.

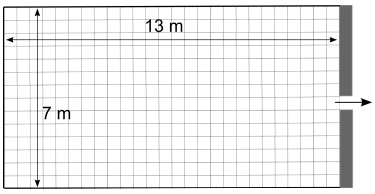

Fig. 1. Experiment was performed in a rectangle room 13 m long and 7 m wide.

2.1 Space

The operational space of the simulation is divided in square-shaped cells with the edge length corresponding to 0.5 m. Each cell $\boldsymbol{x} = (x_{\text{column}}, x_{\text{line}})$ may be either empty or occupied by one agent, which is indicated by the *occupation number* $n(\boldsymbol{x})$, where $n(\boldsymbol{x}) = 0$ if the cell is empty and $n(\boldsymbol{x}) = 1$ otherwise. Here we note, the exit cell $\boldsymbol{e}$ is presented as always empty, keeping the rule that only one agent can enter the cell at the time. Each cell carries the *potential* $U(\boldsymbol{x})$ indicating the attractiveness of the cell for the agent (see [5] for details), which can be defined as

$$U(\boldsymbol{x}) = -F \cdot \varrho(\boldsymbol{e}, \boldsymbol{x}) \ , \tag{1}$$

where F is the constant determining the potential strength and ϱ is a "distance" of the cell $\boldsymbol{x}$ to the exit cell, being often chosen es Euclidian metric, i.e.

$$\varrho(\boldsymbol{e}, \boldsymbol{x}) = \left(|e_{\text{column}} - x_{\text{column}}|^2 + |e_{\text{line}} - x_{\text{line}}|^2\right)^{\frac{1}{2}} \ . \tag{2}$$

For illustration purposes the coordinates of the exit in presented Figures are set to $\boldsymbol{e} = (0, 0)$. To the static properties of the cell belongs the *cell type number* $t(\boldsymbol{x})$, which determines, whether the agent can enter the cell ($t(\boldsymbol{x}) = 1$), e.g. floor cell, exit, or not ($t(\boldsymbol{x}) = 0$), e.g. wall, barrier.

Besides the occupation number, the dynamical status of the cell is determined by the *prediction number* $r(\boldsymbol{x}) \in \{0, 1, \ldots\}$, which denotes the number

of pedestrians being predicted to enter the cell $\boldsymbol{x}$. As we will see in (4), the maximum number of entering agents is 8. The principle of prediction will be explained below.

2.2 Decision Process – Choosing the Target Cell

The essence of the CA dynamics lies in the rules, according to which the agent chooses next target cell. In this project, the agent decides stochastically, i.e. the probability $p_{\boldsymbol{d}}(\boldsymbol{x})$ of choosing the cell $\boldsymbol{x}+\boldsymbol{d}$ from the "target" surrounding $S_T(\boldsymbol{x})$ depends on the current state of the "reaction" surrounding $S_R(\boldsymbol{x})$:

$$p_{\boldsymbol{d}}(\boldsymbol{x}) = \Pr\{\boldsymbol{x}+\boldsymbol{d}|S_R(\boldsymbol{x})\} \quad . \tag{3}$$

In this article, the surrounding according to Moore's definition with range 1 is chosen for both, the target and the reaction surrounding, i.e. $S_T(\boldsymbol{x}) = S_R(\boldsymbol{x}) = \boldsymbol{x} + S_M$, where

$$S_M = \{(-1,1);(0,1);(1,1);(-1,0);(1,0);(-1,-1);(0,-1);(1,-1)\} \tag{4}$$

(see Figure 2). Here, $\boldsymbol{d} \in S_M$ is referred to as *direction*. The definition (4) implies that the agent cannot choose his current position $\boldsymbol{x}$ during the decision process (it does not mean that he *has* to move; see subsection 2.3).

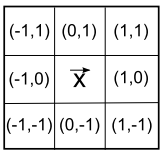

Fig. 2. Moore's surrounding with range 1 of cell $\boldsymbol{x}$, with indexation used in this article.

Let us now denote $\boldsymbol{d}_r(i)$ the currently predicted direction of the agent i. The movement prediction from the view of the agent i then is

$$r'_i(\boldsymbol{d}) = r(\boldsymbol{x}+\boldsymbol{d}) - \delta_{\boldsymbol{d},\boldsymbol{d}_r(i)} \quad , \tag{5}$$

where $\delta_{i,j}$ is the Kronecker's symbol. For all $\boldsymbol{d} \in S_M$ the indicator $\widetilde{r}_i(\boldsymbol{d}) = \delta_{0,r'_i(\boldsymbol{d})}$ indicates, whether the cell $\boldsymbol{x}+\boldsymbol{d}$ is predicted to be entered by another agent than i. Using the notation presented above, the probability that the agent i sitting in the cell $\boldsymbol{x}$ chooses the direction $\boldsymbol{d}$ is given as

$$\begin{aligned} p_{\boldsymbol{d}}(\boldsymbol{x}) = \mathcal{N} \cdot t(\boldsymbol{x}+\boldsymbol{d}) \cdot \exp\{\alpha \cdot U(\boldsymbol{x}+\boldsymbol{d})\} \times \\ \times [1-\beta \cdot n(\boldsymbol{x}+\boldsymbol{d})] \cdot [1-\gamma \cdot \widetilde{r}_i(\boldsymbol{d})] \quad , \end{aligned} \tag{6}$$

where $\mathcal{N}$ is the normalization constant ensuring that $\sum_{\boldsymbol{d}\in U_M} p_{\boldsymbol{d}(x)} = 1$, and coefficients α, β, γ, are coefficients of sensitivity to the potential, occupation number, and prediction number. These parameters are to be determined later and their influence is demonstrated in Figure 3.

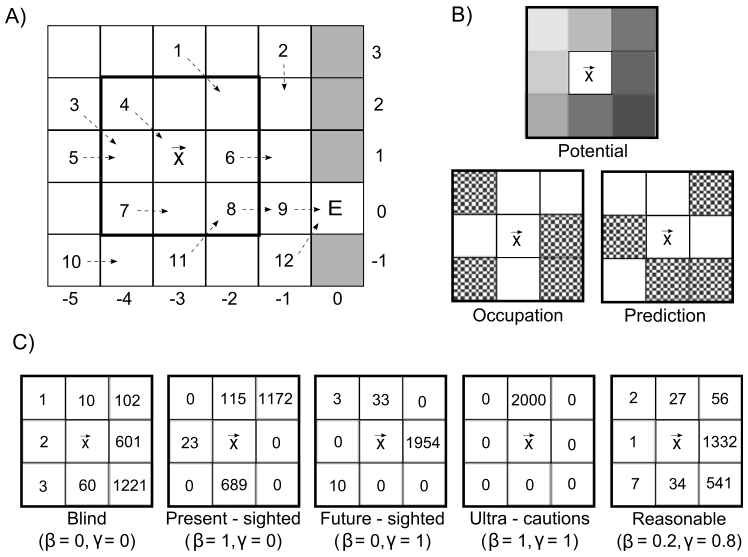

Fig. 3. Example illustrating principle of decision of one pedestrian. Subfigure A visualized wider surrounding of an agent in the cell $\boldsymbol{x}$. Integer numbers represent agents and dashed arrows their predicted movement. The probability distribution $p_{\boldsymbol{d}}(\boldsymbol{x})$ given by (6) is determined by potential, occupation and conflict prediction. The subfigure B visualizes these parameters. The darker color the higher potential (closer to exit), hatched area means penalization in stated category. The final cell attractivity strongly depends on coefficients of sensitivity to stated parameters. While potential represent static conditions, occupation and prediction of conflict reflect agent strategy. Final probabilities for different settings of sensitivity parameters β, γ are shown in subfigure C. For each of them, 2000 decisions were divided into the cells according to (6). The values of potential strength is $F = 3$, and the potential sensitivity $\alpha = 1$. The potential sensitivity plays an important role in the heterogenous system (α_i differs from agent to agent), which is not the demonstrated case.

2.3 Agent Movement and Conflicts

The goal of this subsection is to explain the interaction of all agents within considered time period as a whole. One update of the system can be divided in four phases:

1. Selection of active agents
2. Decision process
3. Conflicts solution and motion
4. Time actualization

1. *Selection of active agents* means that only agents that are supposed to move at the considered time according to their frequency are activated (similar approach has been applied in [14] to handle the diagonal movement symmetrization). Each agent i has its own updating frequency f_i giving the number of

updates during one time unit. In principle, whenever the agent moves, or tries to move, at the time t, the time of his next activation is set to $t + f_i^{-1}$. The only situation, when this rule changes, is after the diagonal movement. Because the diagonal movent (i.e. in directions $(-1, 1)$, $(1, 1)$, $(-1, -1)$, or $(1, -1)$), is $\sqrt{2}$-times longer, it takes $\sqrt{2}$-times more time. This leads to the diagonal movement time-penalization, and the next activation time is set to be $t + qf_i^{-1}$, where q is the rational approximation of $\sqrt{2}$, e.g $q = 3/2$. The rational approximation of $\sqrt{2}$ is necessary, if we want to keep "sufficiently" discrete structure of time for long period.

2. *Decision process* of each agent i proceeds independently and consists in choosing the direction according to given rules explained in section 2.2. If the target cell is empty, the agent is added to the *waiting list* of the cell. If the target cell is occupied by another agent j the *bound* of i to j is created. Agent j is called the *blocker* and agent i becomes *bounded*. The bound holds until the next update of the bounded agent i or until the motion of the blocker j.

3. *Conflict solution and motion.* It is obvious that the two-dimensional structure of the problem connected to the independent decision of agents leads to variety of conflicts.

a) More agents choose the same unoccupied cell (the waiting list of some cell contains more then one agent). In this case, with probability μ, playing role of the *friction parameter* (taken from [13]), the movement of all agents is disabled – non of the agents enters the cell. Otherwise, i.e. with probability $(1 - \mu)$, one of the waiting agents is chosen randomly to enter the cell, the others don't move.

b) The agent chooses an occupied cell. In this case, the agent i predicts the movement of the blocker j and wants to take his place. If the blocker j moves (i.e. is the single agent to enter the target cell or wins the conflict described in a)), the bounded agent i tries to enter his target cell. Again, if he is the only bounded agent to j, there is no conflict. If more then one agent are bounded to j, the occurring conflict is solved analogically to the conflict a). This rule is applied recursively to all bounded agents.

Here we note, that during the conflict solution of type b) even a non-active agent can move, if he is bounded to the blocker. This is illustrated by an example in Figure 4. The principle of conflict solution and bounds during one update is illustrated in Figure 5.

3 Calibration of the Parameters

For parameters calibration, an experiment "leaving the room" was organized. 28 participants were arranged in a room with area 13m × 7m according to specific setting (see fig 6). After initiation, everyone started to move towards the doors.

Participants were only briefly instructed to follow three basic rules:

- leave the room as fast as possible
- do not run, just walk
- avoid physical contact

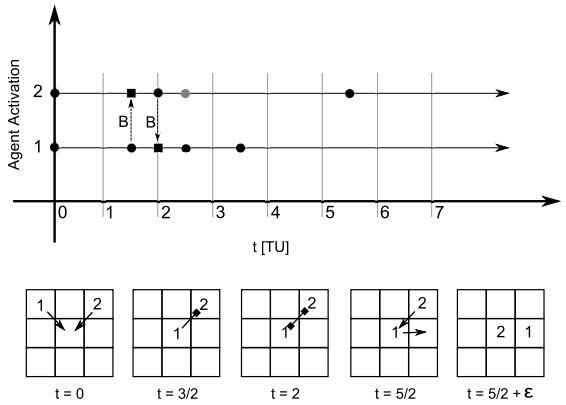

Fig. 4. Example illustrating principle of bounds. Two agents 1 and 2 with frequencies $f_1 = 1$, $f_2 = 1/2$ are activated in time t=0 and decide to enter the same cell $(0, 0)$, agent 1 wins. Next update-time of agent 1 is set to $t = 3/2$ because of the diagonal movement, the agent 2 waits until t=2. At $t = 3/2$ agent 1 decides to enter the cell (1,1) occupied by agent 2 and gets bounded to 2. At $t = 2$ agent 2 decides to enter (0,0) and gets bounded to agent 1. At $t = 5/2$ agent 1 cancels his bound and moves to (1,0). Due to the bound, agent 2 moves to (0,0) and his next-update time is set to $t = 5/2 + 2(3/2)$. The multiplication by 3/2 is due to diagonal movement penalization.

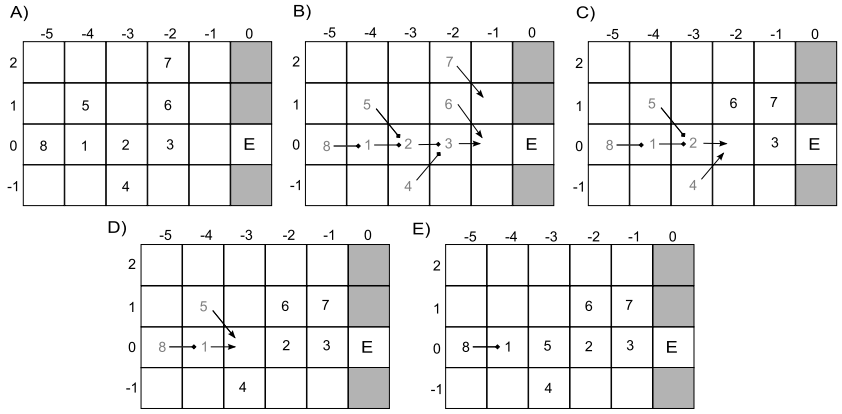

Fig. 5. Example illustrating principle of waiting lists and bounds during one update. 8 agents are depicted at their positions in subfigure A; every agent chooses the target cell and is either added in waiting list (triangles) or bounded to the blocker (squares) as shown in subfigure B. In this case, the agent 7 is in the waiting list of cell (-1,1), agents 3 and 6 in the waiting list of cell (-1,0), agent 4 and 2 are bounded to agent 2 etc.. After conflict solution in waiting lists (subfigure C) the bounds induce conflict in cell (-3,0), which is solved analogically (subfigures D and E).

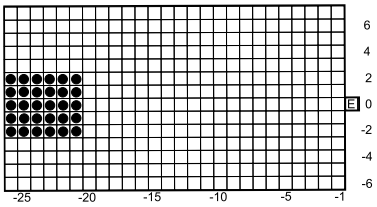

Fig. 6. Initial setting of the experiment, black circles represent pedestrians.

These restrictions protected the participants from injuries, they were not motivated to furious evacuation. Following phenomenons were observed (see left part of Figure 7):

1. Pedestrians hold the initial formation and wait rather than walking around the crowd → occupation is not important ($\beta = 0.2$), but the prediction and bounding principle is significant ($\gamma = 0.8$)
2. Pedestrians are not forced to form a cluster near exit; multi-line (chaotic) queue is formed instead
3. Unsolved conflicts appeared only rarely → low friction parameter μ
4. The movement is relatively deterministic ($F = 3$)

Furthermore, considering the essence of the experiment, strong moral barriers connected to social conventions avoided the participants to create semi-spherical cluster in front of the exit, which is expected in panic-like situations (see e.g. [2], [12], etc.). The participants were not motivated to leave the room earlier than others, therefore there has not been observed any drastic fight at the door. Such behaviour inspired us to deform the spherical form of potential iso-value curves to

$$\varrho(\boldsymbol{e}, \boldsymbol{x}) = \sqrt{\frac{10(e_{\text{line}} - x_{\text{line}})^2}{e_{\text{column}} - x_{\text{column}}} + (e_{\text{column}} - x_{\text{column}})^2} \ . \tag{7}$$

These potential iso-value curves are presented in Figure 8. Here we note that the equation (7) is applicable to define the required potential modification only for normal conditions without obstacles, where the average direction of pedestrian cloud centre towards exit is in the positive x direction. The generalization to more complex geometries requires more detailed experimental study and further discussion.

At the end of experiment, running was allowed. Physical contact was still forbidden, but participants were not able to keep it. These physical forces caused that more than one pedestrian occupied one cell sometimes. On the other hand, expected phenomenons as the spherical shape of cluster near the exit and the inability to hold formation were observed (see right part of Figure 7). The movement under such panic-like conditions is described well using spherical potential (equations (1), (2)). To avoid conflict, runners were quite cautious; both occupation and prediction numbers were significant ($\beta = 0.95$, $\gamma = 0.95$).

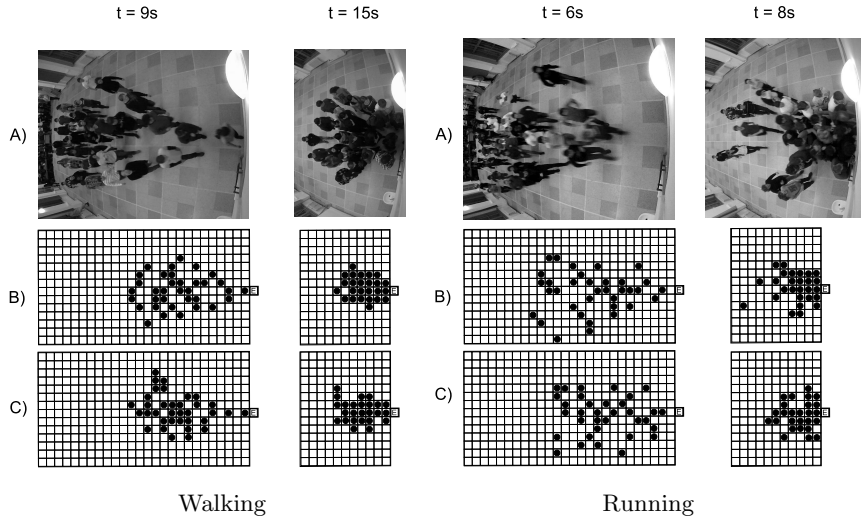

Fig. 7. Visualization of progress of one round, pedestrians walked (left) and run (right). Pictures A come from frontal camera, 9 (resp. 6) seconds after initialization, when first person approaches the exit and 15 (resp. 8) seconds after initialization, when compact cluster is developed. Subfigures B project previous pictures to lattice representation and subfigures C represent corresponding realization of the simulation. One time unit of the simulation corresponds to 0,7 s. The time interval between creating the cluster and completing the evacuation was used to create the time-span of the model, because this article focuses on the shape of the cluster in front of the exit. Mean actualization frequency was set to 1 time unit.

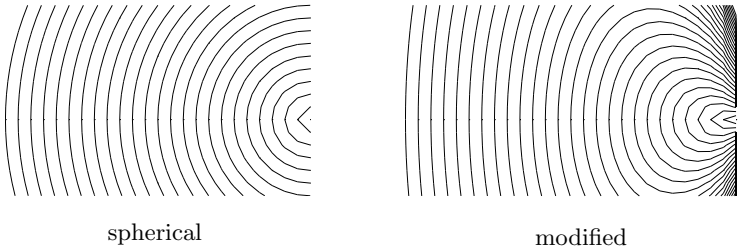

Fig. 8. Demonstration of suggested potential.

4 Conclusion

A concept of CA model of pedestrian crowd modeling has been introduced, which brings new elements in Floor Field model. The principle of waiting list and bounds has been defined. This allows the agent to choose an occupied cell. The innovative idea of creating bound to the blocking agent reflects the observed

line formation and spontaneous queuing typical for the crowd movement with negligible effect of panic. We believe that the proposed mechanism of bounds is very close to the unconscious behaviour of pedestrians in high densities.

The pedestrian velocity is represented by the updating frequency being in this article defined in time discrete way. Nonetheless, it is possible to generalize it in the time continuous way, which meets the presumption that the pedestrian desired velocity is Gaussian distributed.

For the calibration of model parameters the experiment "leave the room" has been performed. Key information has been found to calibrate model parameters to the non-panic simulation of room evacuation. Based on the measured data, the shape of the potential iso-value curves needs to be modified due to the effect of moral barriers connected to social conventions, when the situation is not intensely panic, e.g. controlled evacuation. Proposed rules including bounds and prediction improve the model in spontaneous line formation, but only the simulation with modified potential corresponds to the observed non-spherical shape of the pedestrian cloud in front of the exit.

Here we note that only the macroscopic behaviour represented by the shape and velocity of the pedestrian "cloud" was considered for the calibration of parameters. The microscopic behaviour of single individuals slightly differs from the observed behaviour during the experiment. Although the model has been designed to describe important phenomena of one specific experimental study, we believe that ideas presented here can be used for simulating the movement in more complex situations.

Acknowledgements.

This work was supported by the grant SGS12/197/OHK4/3T/14 and by the MSMT research program under the contract MSM 6840770039. We would like to thank to members of research Group of Applied Mathematics and Stochastics, especially Juraj Panek, for significant help with the experiment preparation and data processing.

References

1. Georgoudas I. G., Koltsidas G., Sirakoulis G. Ch., Andreadis I. Th.: A Cellular Automaton Model for Crowd Evacuation and its Auto-Defined Obstacle Avoidance Attribute. In: Bandini S. et al. (eds.) ACRI 2010. LNCS, vol. 6350, pp. 455 – 464. Springer, Heidelberg (2010)
2. Helbing D., Farkas I., Vicsek T.: Simulating dynamical features of escape panic. Nature 407, 487–490 (2000)
3. Helbing D., Molnar P.: Social force model for pedestrian dynamics. Phys. Rev. E 51/5, 4282–4286 (1995)
4. Henein C. M., White T.: Macroscopic effects of microscopic forces between agents in crowd models. Physica A 373, 694–712 (2007)
5. Kirchner A., Schadschneider A.: Simulation of evacuation processes using a bionics-inspired cellular automaton model for pedestrian dynamics. Physica A 312, 260–276 (2002)

6. Klüpfel H., Schreckenberg M., Meyer-König T.: Models for Crowd Movement and Egress Simulation. In: Traffic and Granular Flow 03, 357–372 (2005)
7. Klüpfel H.: A Cellular Automaton Model for Crowd Movement and Egress Simulation. PhD. thesis, Universität Duisburg-Essen, Germany (2003)
8. Kretz T., Kaufman M., Schreckenberg M.: Counterflow Extension for the F.A.S.T.-Model. In: Umeo H., Morishita S., Nishinari K., Komatsuzaki T., Bandini S. (eds.) Cellular Automata. LNCS, vol. 5191, 555–558. Springer, Heidelberg (2008)
9. Kretz T., Schreckenberg M.: The F.A.S.T. – model. In: Yacoubi S. E., Chopard B., Bandini S. (eds.) ACRI 2006. LNCS, vol. 4173, 712–715. Springer, Heidelberg (2006)
10. Kretz T., Pedestrian Traffic, Simulation and Experiments. PhD. thesis, Universität Duisburg-Essen, Germany (2007)
11. Nishinari K., Kirchner A., Namazi A., Schadschneider A.: Extended floor field CA model for evacuation dynamics. In: IEICE Trans. on Inf. and Syst., vol. E87-D, 726–732 (2004)
12. Schadschneider A., Chowdhury D., Nishinari K.: Stochastic transport in complex systems. Elsevier Science, Amsterdam (2010)
13. Schadschneider A., Seyfried A.: Empirical results for pedestrian dynamics and their implication for cellular automata models. In: Timmermans H., Pedestrian Behavior: models, data collection and applications, Emerald Group Publishing, Bingley (2009)
14. Schultz M., Lehmann S., Fricke, H.: A discrete microscopic model for pedestrian dynamics to manage emergency situations in airport terminals. In: Waldau N., Gattermann P., Knoflacher H., Schreckenberg M. (eds.) Pedestrian and Evacuation Dynamics 2005, 369–375. Springer, Heidelberg (2007)
15. Seyfried A., Portz A., Schadschneider A.: Phase coexistence in congested states of pedestrian dynamics. In: S. Bandini et al. (eds.) ACRI 2010. LNCS, vol. 6350, pp. 496 – 505. Springer, Heidelberg (2010)
16. Steffen B.: A Modification of the Social Force Model by Foresight. In: W. W. F. Klingsch, C. Rogsch., A. Schadschneider, M. Schreckenberg (eds.) Pedestrian and Evacuation Dynamics 2008, 677 – 682. Springer, Heidelberg (2010)
17. Sumaa Y., Yanagisawab D., Nishinari K.: Anticipation effect in pedestrian dynamics: Modeling and experiments. Physica A 391, 248 – 263 (2012)
18. Yamamoto K., Kokubo S., Nishinari K.: Simulation for pedestrian dynamics by real-coded cellular automata (RCA). Physica A 379, 654–660 (2007)